Miniaturization of 90-degree hybrid optical couplers

Miniaturization of 90-degree hybrid optical couplers

Alessio Miranda[1], Weiming Yao[1] , Jos van der Tol[1] and Kevin Williams[1]

[1]Eindhoven University of Technology, De Zaale, Eindhoven, 5612 AZ, The Netherlands
* a.m.d.miranda@tue.nl

Here we explore the limits of miniaturization of an efficient 90-degree hybrid coupler on the InP photonic integration platform, working in the L, C and S bands, with respect to their figures of merit. We investigate the main effects responsible for the degradation of the performance of the devices, and establish the minimal dimension that such devices can have without significant degradation for photonic applications. The miniaturized device has a footprint of only 2200µm^2, more than 5 times smaller than the conventional device used as reference.

Keywords: *multimode interferences MMI, 90-degree hybrid coupler, quadrature hybrid coupler, balanced detector, miniaturization, scaled device, interference*

INTRODUCTION

Multi-mode interferometers (MMI), are a fundamental type of photonic components, whose main function is to distribute the incoming light over several output ports, each with a well-defined power ratio and phase difference with respect to the input [1,2]. The working principle is based on self-imaging caused by internal interference of the modes excited and propagating in it. 90-degree hybrid couplers are a subclass of MMIs, which finds applications in coherent detection systems, where they are used for demodulating optical signals with quadrature phase shift keyed (QPSK) modulation format and in balanced detection [3, 4].

Its structure, depicted in figure 1a, is designed in such way that by applying the received signal S, and a local oscillator (LO) at its input ports, the power at the four outputs is equally distributed, and the phase differences between signal and local oscillator are 0°, ±90°, ∓90° and 180° degrees for each port respectively. In this case, the phase difference between the output channels 1 and 4 (in-phase component) is 0° for the signal and 180° for the local oscillator, while that for the channels 2 and 3 (quadrature component) is 180° and 0° rispectively. The in-phase and quadrature components can be used for balanced detection, allowing for suppression of common mode distortions and improvement of the signal-to-noise ratio.

For large scale integrated circuits, it is required that these devices fit within a densely packed chip. It is thus important to implement strategies for the miniaturization of these devices without compromising their performance. However, the miniaturization of an MMI presents three main challenges: the first is that a reduced size in the input waveguides increases the diffraction effects when the input signals enter the MMI. The second is that crosstalk between input and output waveguides may appear if these are too close. The third is that a reduction of the width of the MMI implies a reduced number of excited and propagating modes inside the MMI which leads to reduced imaging quality. The purpose of this paper is to explore the limits of miniaturization of a working 90-degree hybrid coupler with respect to these challenges and to establish the minimal dimension for which such devices can operate without significant degradation for photonic applications.

DISCUSSION

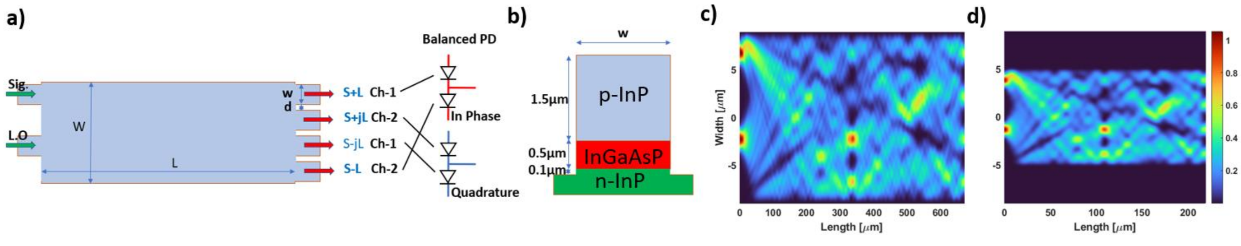

Fig. 1. a) Top view of the hybrid, with output channels and their role in balanced photodetection, b) vertical cross section of the device, c) the intensity distribution in the reference MMI (W=17.8µm, L=671µm, w=3.5µm, d=1µm) with a footprint of almost 12000µm^2 and d) in a miniaturized MMI (W=10.2µm, L=219µm, w=2µm, d=570nm) with a footprint of around 2200µm^2.

The vertical structure of the waveguides and the MMIs in this study, depicted in figure 1b, is a deeply etched rib-waveguide, with a top cladding of 1500nm p-InP (n_u=3.17), a waveguide thickness of 500nm InGaAsP (n_w=3.38), a lower layer of 100nm of n-InP (n_0=3.163) on the same substrate [5]. The device is surrounded by a layer of polyamide (n=1.5). All the simulations are performed using an Eigenmode Expansion Solver (Lumerical MODE-EME), the results refer to the principal TE mode.

The device we chose as reference avoids the restrictions mentioned above: all the waveguides have a width w=3.5µm, to avoid diffraction at the working wavelength (λ =1550nm), the fixed distance between the edges of the output waveguides is d=1µm to avoid cross talking. the Signal and LO input waveguides are indicated in figure 1a. In order to have a correctly working 90 degree hybrid coupler the size of the MMI is chosen to have a W=18µm and $L \approx \frac{4n_{eff}W^2}{3\lambda}$ ≈671µm as calculated in accordance to the literature [1, 2]. By taking into account the effect of the evanescent fields, neglected in [1], we find that the optimal device has a width of W=17.8µm, the other parameters remaining the same as described above. To evaluate the performance of our devices we use four figures of merit at 1550m: the minimum of the moduli of the common mode rejection ratios |CMRR| (as defined in [5]), the maximum of the moduli of the phase errors $|\varepsilon|$ (also defined in [5]), the maximum of the moduli of the excess losses |loss|, and the minimum |Imb| between the moduli of the imbalances in phase and quadrature which we define as $Imb_I = 10\,log(|S_{4S}|^2 - |S_{1S}|^2 - |S_{4LO}|^2 + |S_{1LO}|^2)$ and $Imb_Q = 10\,log(|S_{3S}|^2 - |S_{2S}|^2 - |S_{3LO}|^2 + |S_{2LO}|^2)$.

We consider a miniaturized device as suitable for photonic applications if |CMRR|>20dB, $|\varepsilon| < 5°$, |loss| <1dB and |Imb|>10dB, at the operation wavelength. These conditions are stricter than those which normally apply for a 90-degree hybrid for to be used for balanced detection [6]. For the reference structure, whose images are shown in figures 1c the four figures of merit are |CMRR|=40.2dB, $|\varepsilon| = 0.1°$, |loss| =0.08dB, |Imb|=$24dB$.

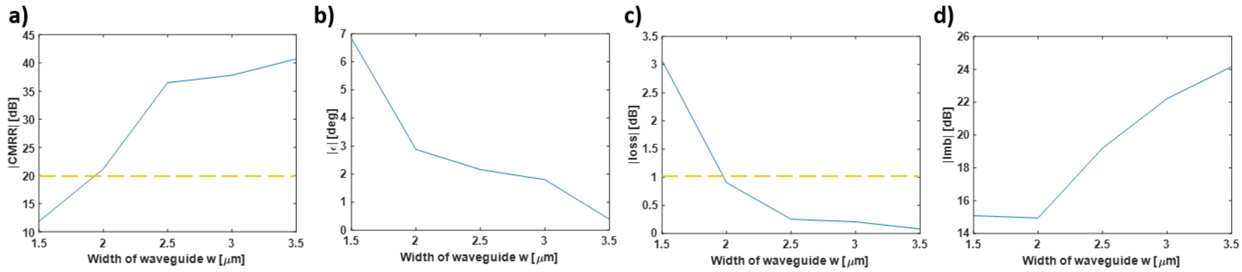

Fig. 2. Comparison of the figures of merit for a) modulus of CMRR, b) modulus of phase error, c) modulus of insertion loss, and modulus of absolute imbalance for devices consisting of the MMI of dimensions (671µm x 17.8 µm) and waveguides scaling from 3.5µm to 1.5µm (the dashed line, when present, indicates the thresholds we set for a suitable device).

In order to explore the effect of diffraction by shrinking the width of the input and output waveguides, we shrink all the waveguides in the reference device, from 3.5µm to 1.5µm by leaving all other dimensions unchanged. As can be seen in figure 2, the device has low degradation for all the figure of merit till a waveguide of 2µm width.

The effect of crosstalk was studied by analysing the S12 of two 100µm long waveguides of width from 1.5µm to 3.5µm separated by 200nm, the minimal distance in the simulation. The length of 100µm is more than sufficient to allow the waveguides to depart from a parallel configuration in a real integrated circuit. In all the examined configurations the calculated cross talk was found to be less than -20dB, which is negligible.

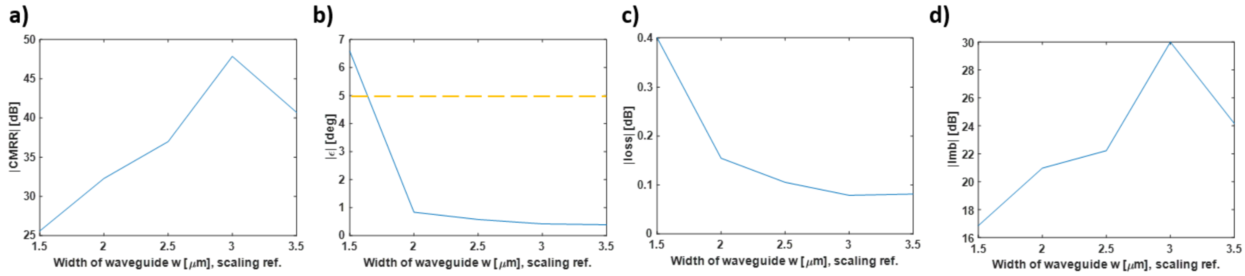

Fig. 3. Comparison of the figures of merit for a) modulus of CMRR, b) modulus of phase error, c) modulus of insertion loss, and modulus of absolute imbalance for devices with waveguides scaling from w_{min}=3.5µm to 1.5µm, and other dimensions scaling accordingly.

Thirdly, we study the dependency of the quality on the number of TE modes excited and propagating in the shrinking MMI. For our devices the number of modes N propagating in the MMI scales as $N = [1.1\ W[\mu m] - 0.48]$.

Because of the geometry of the hybrid, a scaling of the width of the device cannot be independent from the scaling of the waveguides, which must be fully contained in it. Thus we adopt the approach to scale the width of the waveguides w, their relative distance d and width of the MMI W by the same factor α, and to scale the length of the MMI L by α^2 in order to maintain the same proportions as the reference for image formation [1]. This means that the footprint of the MMI scales by α^3. In figure 3 we compare the figures of merit for the miniaturized device depending on the scaling of the waveguide width w_{min}, to which we link the scaling factor of the device as $\alpha = w_{min}/w_{ref}$,where w_{ref}=3.5µm is the width of the waveguide of the reference. We observe that a scaling to $w_{min} = 2\mu m$, corresponding to $\alpha = 0.57$, preserves all the four figures of merit. This corresponds to a miniaturized device with dimensions W=10.2µm, L=219µm, w=2µm, d=570nm and a foodprint of only 2200µm^2.

The intensity distribution, depicted in figure 1d looks very similar to the one of the reference device depicted in figure 1c.

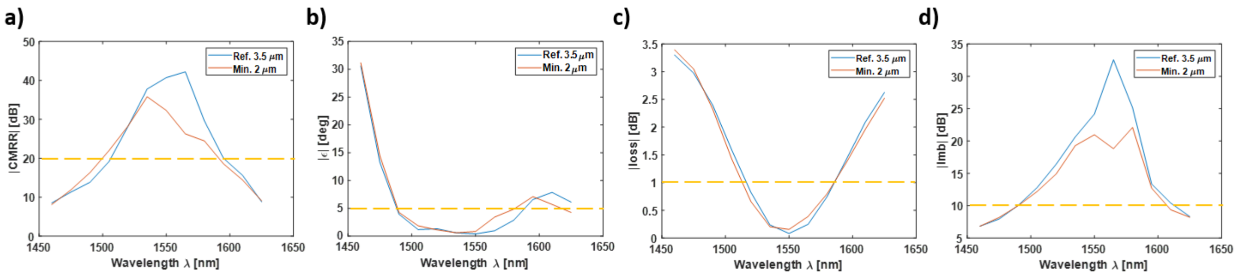

Fig. 4. Comparison of the figures of merit for a) modulus of CMRR, b) modulus of phase error, c) modulus of insertion loss, and modulus of absolute imbalance, in the C, L, S bands.

Finally, in figure 4 we compare the performance of the reference hybrid (w_{ref}=3.5µm, $\alpha = 1$) to the miniaturized one (w_{min}=2µm, $\alpha = 0.57$) for L, C and S band. it can be observed that the devices behave similarly with optimal performance at the working wavelength λ =1550nm, and excellent performance from 1520nm to 1580nm which is the whole C band and part of the L and S bands.

CONCLUSION

In conclusion, we have demonstrated that a standard 90-degree hybrid couple can be scaled from a footprint of 12000µm^2 to one of only 2200µm^2 maintaining a sufficient performance. We compared the principal figures of merit and the behavior in the C, L and S bands for this device and the reference one, This result can prove useful for the integration of these components densely packed photonic circuits.

Acknowledgements: AM would like to thank Ozan Çirkinoğlu, Marco Gagino and Dr. Xaveer Leijtens for fruitful discussion.

References

[1] L. B. Soldano, E. C. M. Pennings, M, *Optical Multi-Mode Interference Devices Based on Self-Imaging : Principles and Applications*, JOURNAL OF LIGHTWAVE TECHNOLOGY, VOL. 13, NO. 4, pp. 615-627,(1995)

[2] K Cooney, FH Peters, *Analysis of multimode interferometers,* Optics express 24 (20), 22481-22515, (2016)

[3] Y. Painchaud, M. Poulin, M. Morin, and M. Têtu, *Performance of balanced detection in a coherent receiver,* Optics Express Vol. 17, Issue 5, pp. 3659-3672 (2009)

[4] B. Zhang, Ch. Malouin, and Th. J. Schmidt, *Design of coherent receiver optical front end for unamplified applications, Optics Express Vol. 20, Issue 3, pp. 3225-3234 (2012)*

[5] E. Kleijn, *Passive components in indium phosphide generic integration technologies.* PhD Thesis, Technische Universiteit Eindhoven, (2014)

[6] OIF-DPC-RX-01.1: Implementation Agreement for Integrated Dual Polarization Intradyne Coherent Receivers, Optical Internetworking Forum Std., April (2010)